University of Groningen

Iron and mixing affect biological carbon uptake in SOIREE and EisenEx, two Southern Ocean iron fertilisation experiments

Bakker, Dorothee C.E.; Bozec, Yann; Nightingale, Philip D.; Goldson, Laura; Messias, Marie-José; Baar, Hein J.W. de; Liddicoat, Malcolm; Skjelvan, Ingunn; Strass, Volker; Watson, Andrew J.

IMPORTANT NOTE: You are advised to consult the publisher's version (publisher's PDF) if you wish to cite from it. Please check the document version below.

Document Version
Publisher's PDF, also known as Version of record

Publication date:
2005

Link to publication in University of Groningen/UMCG research database

Iron and mixing affect biological carbon uptake in SOIREE and EisenEx, two Southern Ocean iron fertilisation experiments

Dorothee C.E. Bakker[a,*], Yann Bozec[b], Philip D. Nightingale[c], Laura Goldson[a,c], Marie-José Messias[a], Hein J.W. de Baar[b], Malcolm Liddicoat[c], Ingunn Skjelvan[d], Volker Strass[e], Andrew J. Watson[a]

[a]School of Environmental Sciences, University of East Anglia, Norwich NR4 7TJ, UK
[b]Royal Netherlands Institute for Sea Research, 1797SK Den Hoorn (Texel), The Netherlands
[c]Plymouth Marine Laboratory, Prospect Place, West Hoe, Plymouth PL1 3DH, UK
[d]Geophysical Institute, University of Bergen, Allégaten 70, 5007 Bergen, Norway
[e]Alfred Wegener Institute for Polar and Marine Research, P.O. Box 120161, 27515 Bremerhaven, Germany

Abstract

This study explores the changes in the surface water fugacity of carbon dioxide (fCO_2) and biological carbon uptake in two Southern Ocean iron fertilisation experiments with different hydrographic regimes. The Southern Ocean Iron Release Experiment (SOIREE) experiment was carried out south of the Antarctic Polar Front (APF) at 61°S, 141°E in February 1999 in a stable hydrographic setting. The EisenEx experiment was conducted in a cyclonic eddy north of the APF at 48°S, 21°E in November 2000 and was characterised by a rapid succession of low to storm-force wind speeds and dynamic hydrographic conditions. The iron additions promoted algal blooms in both studies. They alleviated algal iron limitation during the 13-day SOIREE experiment and probably during the first 12 days of EisenEx. The fCO_2 in surface water decreased at a constant rate of 3.8 µatm day^{-1} from 4 to 5 days onwards in SOIREE. The fCO_2 reduction was 35 µatm after 13 days. The evolution of surface water fCO_2 in the iron-enriched waters (or 'patch') displayed a saw tooth pattern in EisenEx, in response to algal carbon uptake in calm conditions and deep mixing and horizontal dispersion during storms. The maximum fCO_2 reduction was 18–20 µatm after 12 and 21 days with lower values in between. The iron-enriched waters in EisenEx absorbed four times more atmospheric CO_2 than in SOIREE between 5 and 12 days, as a result of stronger winds. The total biological uptake of inorganic carbon across the patch was 1389 ton C ($\pm 10\%$) in SOIREE and 1433 ton C ($\pm 27\%$) in EisenEx after 12 days (1 ton = 10^6 g). This similarity probably reflects the comparable size of the iron additions, as well as algal growth at a similar near-maximum growth rate in these

---

*Corresponding author. Tel.: +44 1603 592648; fax: +44 1603 591327.
E-mail address: D.Bakker@uea.ac.uk (D.C.E. Bakker).

regions. The findings imply that the different mixing regimes had less effect on the overall biological carbon uptake across the iron-enriched waters than suggested by the evolution of fCO$_2$ in surface water.

1. Introduction

The availability of light, nutrients, and trace elements, as well as grazing pressure, influence phytoplankton growth and carbon cycling in the oceans. High-Nutrients Low-Chlorophyll (HNLC) regions have low chlorophyll concentrations, despite high concentrations of nitrate, silicate, and phosphate. Recent experiments have demonstrated that iron is an important, but not the only, limiting factor for algal growth in HNLC regions (See De Baar and Boyd, 2000). Four Lagrangian, *in situ* iron fertilisation experiments have been carried out in the Southern Ocean to date: the Southern Ocean Iron Release Experiment (SOIR-EE), EisenEx and the SOFeX north and south experiments. Iron addition promoted development of an algal bloom, build-up of biomass, and uptake of inorganic carbon (Boyd et al., 2000; Watson et al., 2000; Smetacek, 2001; Gervais et al., 2002; Coale et al., 2004; Bozec et al., 2005). Carbon export increased in the two SOFeX experiments (Buesseler et al., 2004).

An increase in carbon export upon iron addition corresponds to the equivalent storage of the greenhouse gas carbon dioxide (CO$_2$) on time scales of a few months to thousands of years. Therefore, iron fertilisation has been suggested as a tool to reduce the atmospheric CO$_2$ concentration (Martin, 1990). However, iron fertilisation of the oceans for mitigating global warming is controversial. The magnitude and duration of carbon storage remain uncertain and direct verification of the carbon storage is virtually impossible (Gnanadesikan et al., 2003). Iron fertilisation experiments demonstrate that carbon storage is less efficient than assumed in geo-engineering proposals (Boyd et al., 2004). A modelling study suggests that remineralisation of exported organic carbon in the water column, and long-term effects of nutrient depletion on export production may drastically reduce the potential for carbon storage (Gnanadesikan et al., 2003). In addition, iron fertilisation is likely to have negative side effects, such as the marine production of the greenhouse gases nitrous oxide (N$_2$O), and methane (CH$_4$) (Fuhrman and Capone, 1991; Law and Ling, 2001; Jin and Gruber, 2003), and of dimethyl sulphide, alkyl nitrates, and halocarbons (Turner et al., 1996, 2004; Chuck, 2002; Chuck et al., 2002). Large-scale iron fertilisation would promote major changes in marine ecology and marine biogeochemical cycles (Chisholm et al., 2001).

Here, we will present the evolution of surface water fugacity of CO$_2$ (fCO$_2$) in the EisenEx experiment. This study complements the description of changes in dissolved inorganic carbon (DIC) in Bozec et al. (2005). We will quantify the biological uptake of DIC in the mixed layer across the iron-enriched waters (patch) and in the centre of the patch. This article will compare changes in inorganic carbon chemistry in EisenEx with those in SOIREE (Watson et al., 2000; Bakker et al., 2001). The study will explore how the meteorological and hydrographic conditions affected biological carbon uptake upon iron fertilisation (Table 1).

2. Methods

2.1. The SOIREE experiment

The SOIREE experiment was carried out for 13 days in austral summer (9–22 February 1999) (Fig. 1; Table 1). After an initial site survey, the R.V. *Tangaroa* sailed along a spiralling track, while releasing iron and an inert tracer, SF$_6$ (sulphur hexafluoride). An iron-enriched patch of

Table 1
Main features of the SOIREE and EisenEx iron experiments

Feature	SOIREE	EisenEx
Location	61°S, 141°E; Indian sector; south of the APF (1)	48°S, 21°E; Atlantic sector; between the SAF and the APF; in a cyclonic eddy shed by the APF (2, 3, 4)
Timing	Summer; 09–22/02/1999; 13 days; 42 days in SeaWiFS (5)	Spring; 07–29/11/2000; 22 days
Iron addition	0, 3, 5, 7 days; 1745 kg Fe (768, 312, 312, 353 kg) (6)	0, 8, 16 days; 2340 kg Fe (3×780 kg) (7)
Meteorology	Storms after 1 and 4 days; overcast	Succession of storms (5, 13 days) and low wind events; overcast periods and sunny spells
Mixed layer	60–80 m deep (8)	14–100 m deep (4, 9); occasional diurnal stratification
Patch	Low shear; horizontal advection 7% day^{-1}, stretching (5)	Strong horizontal dispersion; initial doubling of size in 4–5 days; distortion; rotation (10)
Surface water fCO$_2$ decrease	From 4 to 5 days onwards at a rate of 3.8 µatm day^{-1}; 32–38 µatm in 13 days; top hat effect for 13 days (11)	From 4 to 7 days onwards; irregular saw tooth: 18–20 µatm after 12 and 21 days with lower values in between; possible top hat effect for 12 days (12)
DIC reduction	15–18 µmol kg^{-1} in 13 days; across the upper 50 m (11)	12–15 µmol kg^{-1} in 22 days; occasional DIC gradients in the mixed layer (12, 13)

Abbreviations are SAF: Subantarctic Front, APF: Antarctic Polar Front. Numbers refer to: (1) Boyd et al. (2000); (2) Smetacek (2001); (3) Strass et al. (2001); (4) Cisewski et al. (2005); (5) Abraham et al. (2000); (6) Bowie et al. (2001); (7) De Baar (2001); (8) Law et al. (2003); (9) Goldson (2004); (10) Watson et al. (2001); (11) Bakker et al. (2001); (12) This study; and (13) Bozec et al. (2005).

~50 km^2 was created at 61°S, 141°E, south of the Antarctic Polar Front (APF) (Boyd et al., 2000). Iron was added a further three times (Fig. 2). The total addition of iron was 1745 kg (Bowie et al., 2001). The iron additions theoretically increased the surface water iron concentration to 3.8, 2.7, 2.6, and 2.5 nM in the successive iron releases (Bowie et al., 2001). These concentrations were approximately ten-fold higher than the concentrations of dissolved iron (0.1 nM) and total iron (0.4 nM) in non-fertilised waters.

2.2. The EisenEx experiment

The EisenEx experiment (cruise ANT 18-2 of R.V. *Polarstern*) took place for 22 days in austral spring (8–30 November 2000) (Fig. 1; Table 1). An iron-enriched patch tagged with SF$_6$ was created in a cyclonic eddy at 48°S, 21°E, north of the APF (Smetacek, 2001; Strass et al., 2001; Cisewski et al., 2005). The characteristics of the eddy water denoted an APF origin. In total, 2340 kg of iron was released in three additions (Fig. 3) (De Baar, 2001).

2.3. Studying the iron-enriched waters in SOIREE and EisenEx

In both experiments, SF$_6$ was used to distinguish the waters inside and outside the iron-enriched patch, while taking SF$_6$ as a proxy for the added iron. Mapping of the surface water expression of the patch was carried out repeatedly for several parameters, notably for SF$_6$, dissolved iron, and fCO$_2$. The ship's continuous surface water supply was at 5 m (SOIREE) and 11 m depth (EisenEx). Water temperature and salinity were registered near the water intake. Regular CTD casts were taken inside and outside the patch. Samples for biological and chemical parameters were taken from the Niskin bottles on the CTD rosette.

The ship's GPS position was corrected for Lagrangian drift. In SOIREE, the correction was based on ADCP measurements (courtesy of Ed Abraham, NIWA). For EisenEx a drift correction for the main mapping periods was based on drifting buoys with a drogue at 20–30 m depth and ADCP measurements (courtesy of Boris Cisewski, AWI). Times (in days) were adjusted
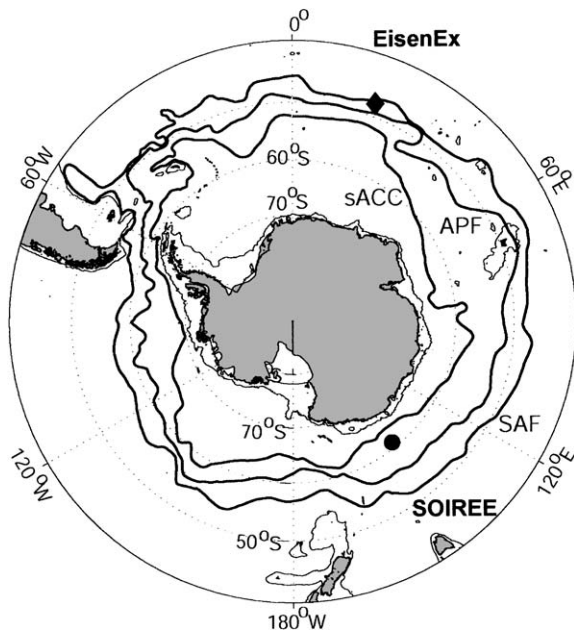
Fig. 1. The location of the SOIREE (circle) and EisenEx (diamond) experiments in the Southern Ocean. The approximate position of the circumpolar Subantarctic Front, the Antarctic Polar Front (APF), and the Southern ACC Front has been indicated (thick lines) (after Orsi et al., 1995), as well as land (grey) and the 1000 m depth contour (thin line) (from ETOPO 5, 1988).

relative to the midpoint of the first iron addition: 9 February 1999, 12:00 UTC in SOIREE and 8 November 2000, 00:00 UTC in EisenEx.

Sensors on the ships routinely measured meteorological parameters, such as air temperature, wind speed, and wind direction. Atmospheric pressure was corrected to sealevel. Wind speed was measured at 15 m (SOIREE) and 37 m height (EisenEx) above the sea surface and was corrected to 10 m height, while assuming neutral boundary conditions. For SOIREE a factor of 0.96 was used. A factor of 0.87–0.90 was calculated for 10 min wind speed with formulae by Large and Pond (1981) for EisenEx.

2.4. Sulphur hexafluoride analysis

Semi-continuous analysis of the surface water concentration of SF_6 was carried out. Water from the ship's surface water supply was pumped directly into the continuous SF_6 mapping system
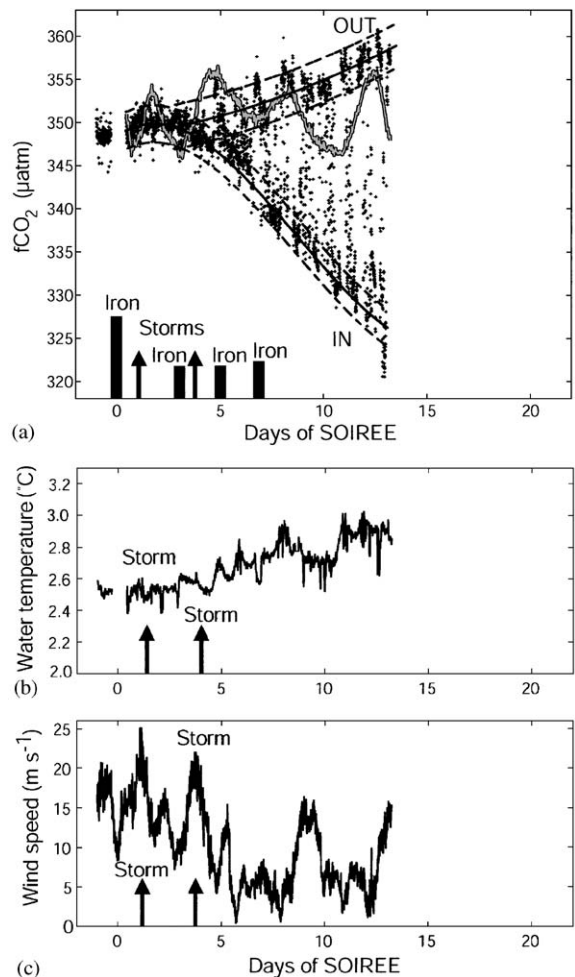

Fig. 2. (a) The evolution of fCO_2 in surface water ($+$, individual measurements) and air (grey line) in SOIREE. The lines indicate fits of fCO_2 at the 10% lowest (upper line) and highest (lower line) SF_6 concentrations for each day (Watson et al., 2000; Bakker et al., 2001). The dashed lines correspond to 84% and 74% of the root mean square error of the fits, respectively. Black bars indicate the timing and the relative size of the iron additions. The arrows point to the occurrence of storms. (b) Water temperature at 5 m depth, and (c) wind speed.

(Watson et al., 2001; Law et al., 2003). Dissolved SF_6 was stripped from the water, trapped cryogenically, separated from oxygen and quantified by a gas chromatograph with an Electron Capture Detector. Every 195 s a measurement was made and time stamped by GPS. The time delay between sampling and analysis was 5–8 min.

2.5. The fCO_2 in surface water and marine air

Online measurements of fCO_2 in surface water and marine air were made throughout SOIREE (Watson et al., 2000; Bakker et al., 2001) and EisenEx with similar techniques. Marine air was collected through tubing from the crow's nest. Seawater from the ship's surface water supply was introduced into a fast response equilibrator with a showerhead. A Pt-100 sensor accurately monitored the temperature of the water in the equilibrator. Every 4 min an infrared LI-COR 6262 analyser determined the mixing ratios of CO_2 and moisture in a sample from the equilibrator headspace or from marine air. Samples were dried before analysis in EisenEx, but not in SOIREE. Two secondary CO_2 standards, which had been calibrated against three certified NOAA standards
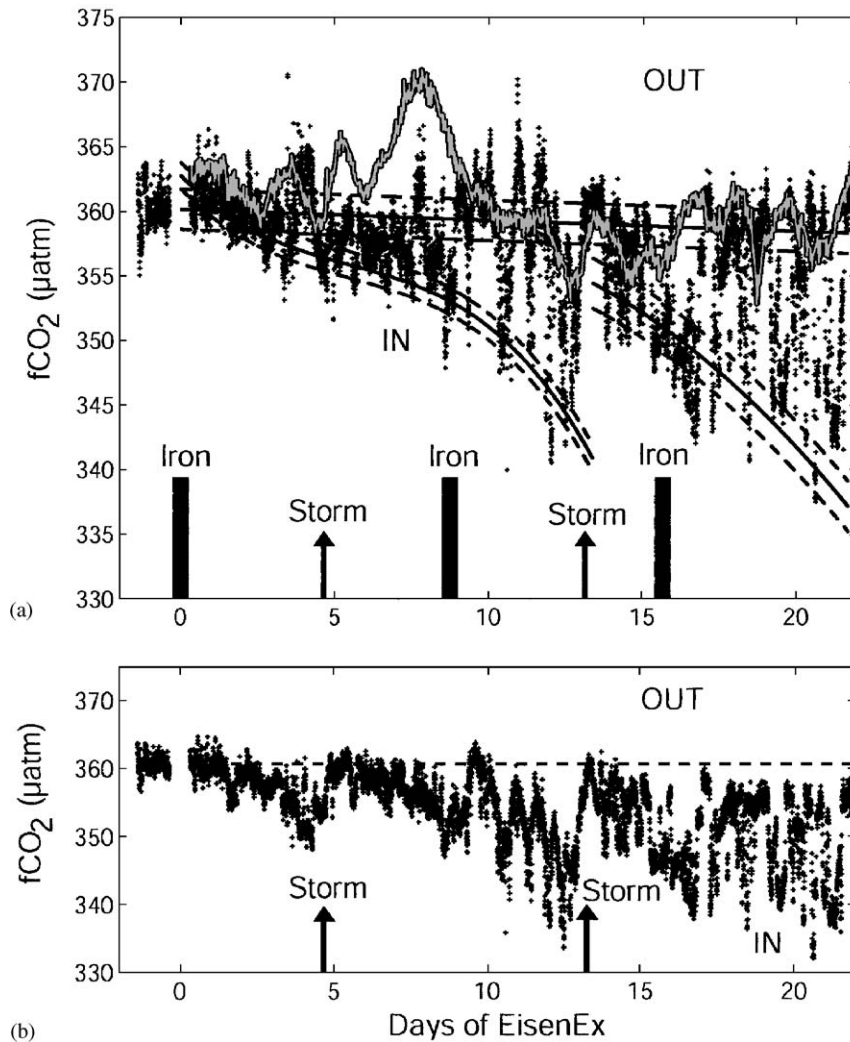

Fig. 3. (a) The evolution of fCO_2 in surface water (+) and air (grey line) in EisenEx with fits of fCO_2 at the 5% lowest (upper line) and highest (lower line) SF_6 concentrations for successive periods. The dashed lines correspond to 84% and 74% of the root mean square error of the fits. Black bars indicate the timing and the relative size of the iron additions. Arrows indicate the occurrence of storms. (b) Surface water fCO_2 corrected to 3.6 °C (+), average atmospheric fCO_2 (dashed line), (c) water temperature at 11 m depth, (d) wind speed, and (e) the mixed layer depth for a density change of $0.02 \, kg \, m^{-3}$ at CTD stations inside the patch (Goldson, 2004).
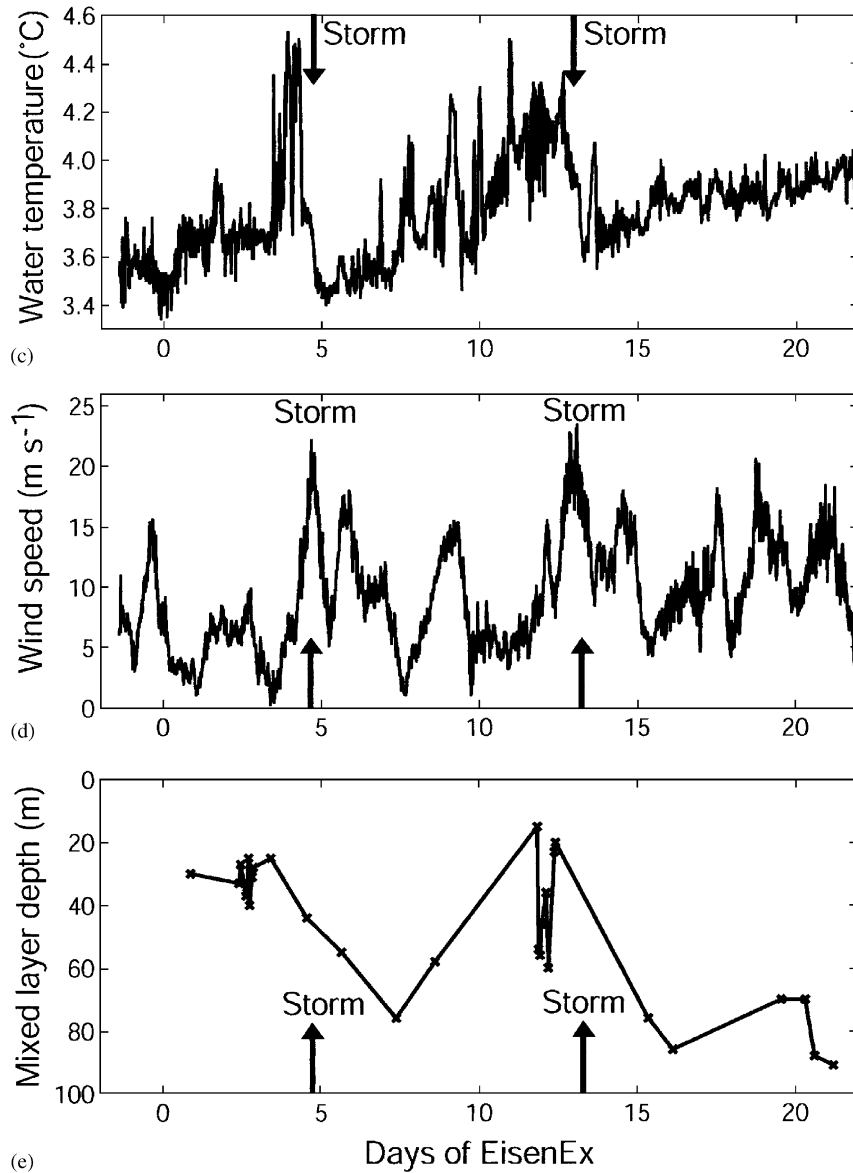
Fig. 3. (*Continued*)

($\sim$250, 350, 450 μmol mol^{-1}), were analysed every 45 min. The secondary standards had CO_2 mixing ratios of 206.5, 512.5 (SOIREE), 295.1, and 406.1 μmol mol^{-1} (EisenEx) with an accuracy better than 0.6 μmol mol^{-1}. The relationship between the LI-COR readings (in μmol mol^{-1}) and the mixing ratios of the NOAA standards was linear with an accuracy of 0.2 μmol mol^{-1}. The

zero and span of the instrument were not changed during the cruises. Average warming of the water between the seawater inlet and the equilibrator was 0.5 °C in SOIREE and 0.2 °C (standard deviation $\sigma = 0.1$ °C for 8362 values) in EisenEx. The equation by Takahashi et al. (1993) was used to correct for the warming. The fCO$_2$ measurements were time stamped by a GPS sensor. The

time delay between sampling and analysis was 4 min for fCO_2 in air and surface water.

The precision and accuracy of surface water fCO_2 and the mixing ratio of atmospheric CO_2 in SOIREE were estimated as 0.6, 1.0 µatm (1 µatm = 0.101325 Pa), 0.6, and 1.0 µmol mol^{-1}, respectively (Bakker et al., 2001). We assume that these values for surface water fCO_2 also apply in EisenEx. A comparison of atmospheric CO_2 mixing ratios during EisenEx with independent data suggests a precision and an accuracy better than 0.6 µmol mol^{-1} (Section 3).

2.6. Dissolved inorganic carbon

The concentration of DIC was determined on samples from regular CTD casts inside and outside the patch (Bakker et al., 2001; Bozec et al., 2005). In SOIREE, samples were also taken from the ship's surface water supply. Samples were collected in 250 ml (SOIREE) and 1000 ml (EisenEx) glass bottles. The samples were kept cold before measurement in water from the continuous sea-water supply. The DIC concentration was determined by the coulometric method of Johnson et al. (1993). Three replicate analyses were made on each sample. A DIC seawater standard (DOE, 1994) was measured for each coulometric cell. Precision and accuracy were estimated as better than 2.7 µmol kg^{-1} in SOIREE (Bakker et al., 2001) and as 2.0 µmol kg^{-1} in EisenEx (Bozec et al., 2005).

2.7. Spatial interpolation of surface water fCO$_2$

Surface water fCO_2 was interpolated for mapping periods on a 0.5 km × 0.5 km grid by Ordinary Kriging for SOIREE (Bakker et al., 2001) and EisenEx (Fig. 4). This interpolation method for irregularly spaced data expresses the spatial correlation between the data in a semi-variogram (Journel and Huijbregts, 1977; Bailey and Gatrell, 1995). Ordinary Kriging provides the best linear unbiased estimate. The interpolation was performed with the program Easy_Krig versions 1.0 (SOIREE) and 2.1 (EisenEx) (courtesy of Dezhang Chu, Woods Hole Oceanographic Institution). An exponential cosine function type 1 was fitted to the

semi-variogram. Interpolated fCO_2 was used if the standard deviation of the fitting error did not exceed the standard deviation of the data. Surface water fCO_2 had been drift corrected prior to the interpolation. No Lagrangian drift correction was available for 17.8–18.8 days in EisenEx. Sea surface temperature varied little during the mapping periods ($\sigma \leqslant 0.1\,^\circ$C in EisenEx).

Fits were made between surface water fCO_2 and the 5% (EisenEx) or 10% (SOIREE) highest or lowest SF_6 values for successive periods. The fits indicate which waters had been enriched in iron and SF_6 (Figs. 2 and 3; Table 2). Bakker et al. (2001) provide details of the fits for SOIREE. Use of a 5% or 10% criterion for EisenEx did not greatly affect estimates of the net DIC change (Section 2.8) across the patch (+2%) and reduced the net DIC change in the patch centre after 18 days by 14%. The 5% setting gave a slightly more accurate fit than 10%. For EisenEx, fits with fCO_2 corrected to 3.6 $^\circ$C rather than fCO_2 had low accuracy. Table 3 lists the criteria used for defining which grid points on the fCO_2 maps were inside the patch and in the patch centre (Bakker et al., 2001). 'Background fCO_2' was calculated from the fit of fCO_2 to the 10% (SOIREE) and 5% (EisenEx) lowest SF_6 values.

2.8. Integration of DIC changes

2.8.1. Net changes in DIC

Net changes in DIC (ΔDIC_{fCO_2}) were calculated for the mixed layer of the patch and the patch centre by using the fCO_2 maps (Fig. 4; Table 3) (Bakker et al., 2001). A fit between surface water fCO_2 and DIC in the upper 20 m was made for SOIREE. Details of the fit are in Table 3 and Bakker et al. (2001). Warming of the water during EisenEx (Fig. 3) was taken into account by using surface water fCO_2 corrected to 3.6 $^\circ$C, rather than fCO_2, in the fit (Tables 3 and 4). The DIC change at a grid point was taken as the difference between DIC corresponding to fCO_2 at that grid point and DIC at background fCO_2 in SOIREE, while both fCO_2 values had been corrected to 3.6 $^\circ$C in EisenEx (Table 3).

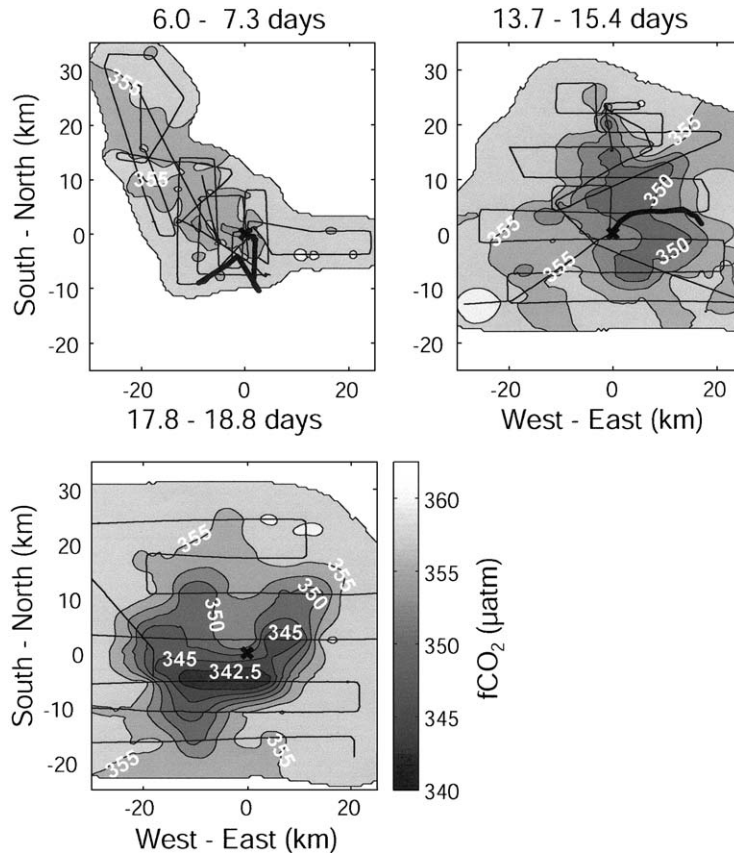The vertically integrated change in DIC at the grid points was obtained by multiplication of the

Fig. 4. The spatial distribution of surface water $f\mathrm{CO}_2$ for mapping periods (in days) in EisenEx. Surface water $f\mathrm{CO}_2$ measurements along the ship's track (thin line) were interpolated to a 0.5 km by 0.5 km grid by Kriging. The contour lines are at 2.5 µatm intervals from 342.5 to 362.5 µatm. The thick line shows the trajectory of the Lagrangian buoy with a cross for its departure point.

Table 2
Fits for surface water $f\mathrm{CO}_2$ in EisenEx at the 5% lowest and highest SF_6 as a function of time with the equation $f\mathrm{CO}_2 = a_3 t^3 + a_2 t^2 + a_1 t + a_0$, correlation coefficient r and root mean square error (RMS)

	Lowest 5%	Highest 5% (1)	Highest 5% (2)
a_3	0	−0.0200	0
a_2	0	0.331	−0.098
a_1	−0.085	−2.475	1.344
a_0 (µatm)	360.1	362.7	353.9
r	−0.24	−0.89	−0.76
RMS (µatm)	1.9	1.4	2.6
Number	184	124	78
Period (days)	0.0–18.8	0.0–11.5	13.7–18.8

Fits (1) and (2) at the 5% highest SF_6 correspond to the periods before and after the second storm (Fig. 3).

surface water DIC change with a 50 m depth interval for SOIREE, as changes in DIC uniformly occurred in the upper 50 m, but not below 50 m depth (Bakker et al., 2001). The net DIC change across the mixed layer was calculated for EisenEx by multiplying the surface water DIC change with the mixed layer depth and a factor 0.8, as DIC changes in the lower part of the mixed layer were often lower than in surface water (Fig. 5) (Bozec et al., 2005). The mixed layer depth was calculated from a $0.02\,\mathrm{kg\,m^{-3}}$ change in potential density from the sea surface in EisenEx (Goldson, 2004). This criterion gave mixed layer depths, which corresponded to the maximum depth with DIC uptake (Fig. 5). The addition of the vertically integrated DIC change at the grid points provided

Table 3
Calculation of DIC changes for the mixed layer of the patch and the patch centre in SOIREE (Bakker et al., 2001) and EisenEx

	SOIREE	EisenEx
Surface water fCO_2	Drift correction; Kriging $0.5\,km \times 0.5\,km$	Drift correction, except 17.8–18.8 days; Kriging $0.5\,km \times 0.5\,km$
Background fCO_2	Fit of fCO_2 at 10% lowest SF_6	Fit of fCO_2 at 5% lowest SF_6
In the patch	$fCO_2 \leqslant fCO_{2L} - 84\%\ RMS_L$	$fCO_2 \leqslant fCO_{2L} - 84\%\ RMS_L$
Patch center	$fCO_2 \leqslant fCO_{2H} + 74\%\ RMS_H$	$fCO_2 \leqslant fCO_{2H} + 74\%\ RMS_H$
Warming	No correction	Correction of fCO_2 maps to $3.6\,°C$
Surface ΔDIC	$\Delta DIC = 0.43\Delta fCO_2 + 1984.1$	$\Delta DIC = 0.50\Delta fCO_{2\_3.6\,°C} + 1948.8$
ΔDIC over depth	Surface ΔDIC across $50\,m$ depth	Surface ΔDIC for the mixed layer depth and a factor 0.8
Vertical diffusion	$K_z = 0.11 \pm 0.2\,cm^2\,s^{-1}$ (1); $\Delta z = 50$–$90\,m$	$K_z = 0.54 \pm 0.77\,cm^2\,s^{-1}$ (2); Δz from 80% of the mixed layer depth to $120\,m$

Fits of surface water fCO_2 to the 5% or 10% lowest (L) or highest (H) SF_6 concentrations for successive periods (Figs. 2 and 3) help distinguish where fCO_2 grid points are relative to the patch. RMS is the root mean square error of such a fit. Details of the fits are in Tables 2 and 4 (EisenEx) and in Bakker et al. (2001) (SOIREE). Numbers refer to: (1) Law et al. (2003); (2) Goldson (2004).

Table 4
Fits for surface water fCO_2 at $3.6\,°C$ (A) and surface water fCO_2 (B) to DIC in the upper $20\,m$ depth in EisenEx with the equations $DIC = a_1 fCO_{2\_3.6\,°C} + a_0$, $DIC = a_1 fCO_2 + a_0$, correlation coefficient r and the root mean square error (RMS)

	A for $fCO_{2\_3.6\,°C}$	B for fCO_2
a_1	0.50	0.54
a_0	1948.8	1931.6
r	0.91	0.82
RMS ($\mu mol\,kg^{-1}$)	2.0	2.8
Number	24	24
Period (days)	4.5–22.0	4.5–22.0

Fit A was used in the standard scenario, while B was used for determining the robustness of the estimates.

the total net DIC change (ΔDIC_{fCO_2}) across the patch. The average DIC change across the mixed layer was calculated for the patch centre.

The accuracy of the net DIC reduction (ΔDIC_{fCO_2}) was obtained by repeating the above procedure for different assumptions. Bakker et al. (2001) describe this procedure for SOIREE. The accuracy of ΔDIC_{fCO_2} in EisenEx was calculated by using six additional scenarios with different criteria for the interpolation of surface water fCO_2 (linear interpolation), for the fit of fCO_2 at $3.6\,°C$ against DIC (fCO_2 rather than fCO_2 at $3.6\,°C$), for the intensity of the DIC change in the mixed layer (factors of 0.6 and 1.0), and for the characterisa-

tion of the patch and the patch centre (fCO_2 at 10% highest SF_6 and 100% of RMS). These scenarios changed the net DIC reduction across the patch after 18 days by -4%, $+10\%$, -25%, $+25\%$, $+2\%$, and -3%, respectively. The uncertainty due to the mapping scenario was defined as the standard deviation of the net DIC change in the seven scenarios.

2.8.2. Air–sea exchange of CO_2

The effect of CO_2 air–sea transfer on DIC (ΔDIC_{AirSea}) was calculated for the patch and the patch centre. Eq. (1) was used to estimate the air–sea flux (F_{AirSea}) from fCO_2 at grid points, and averages of wind speed, atmospheric fCO_2, water temperature, and salinity for each mapping period:

$$F_{AirSea} = kK_0(fCO_{2water} - fCO_{2air}) \quad (1)$$

with transfer velocity (k) and solubility (K_0). The skin temperature was taken equal to the bulk water temperature. The quadratic relationship for short term, shipboard wind speed by Wanninkhof (1992) was used for the calculation of the gas transfer velocity from average wind speed. Addition and averaging of the fluxes at the grid points provided the air–sea flux for the patch and the patch centre, respectively. The effect of air–sea exchange on DIC over time was calculated by interpolation of the flux between successive mapping periods. The error in ΔDIC_{AirSea} has been
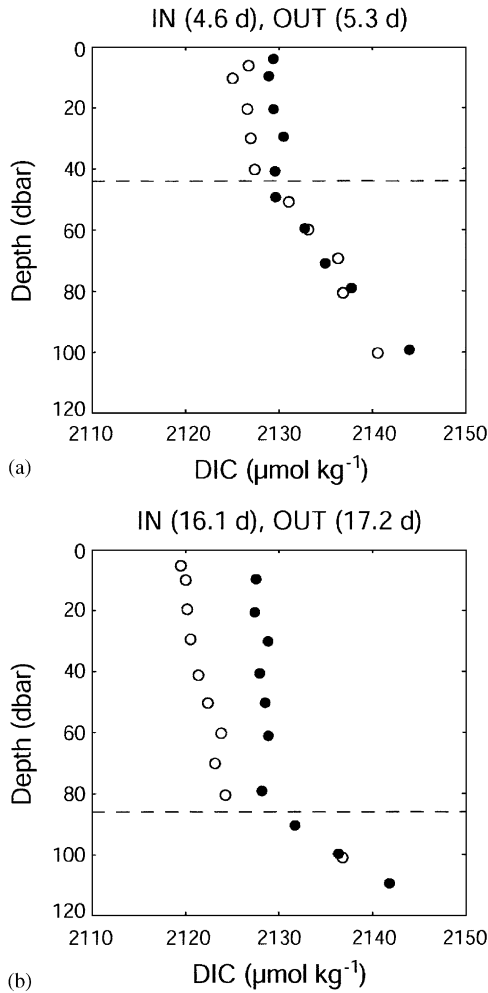
Fig. 5. The vertical distribution of DIC at CTD stations in the patch centre ('IN', open circles) and outside the patch ('OUT', closed circles). The dashed line indicates the mixed layer depth at the IN stations from the $0.02\,\mathrm{kg\,m^{-3}}$ density criterion (Goldson, 2004). The timing of the casts is in days (d).

taken as 55%, reflecting uncertainty in the gas transfer velocity (50%) (Liss and Merlivat, 1986; Wanninkhof and McGillis, 1999; Nightingale et al., 2000) and from the mapping scenarios (5%).

2.8.3. Vertical diffusion

Vertical diffusion (F_{VDif}) of DIC across the pycnocline was calculated from the change in DIC (ΔDIC) over depth (Δz) and the vertical diffusivity

K_z with the equation:

$$F_{\mathrm{VDif}} = -K_z\,\Delta\mathrm{DIC}/\Delta z. \qquad (2)$$

The vertical diffusivity was $0.11\,\mathrm{cm^2\,s^{-1}}$ ($\pm 0.2\,\mathrm{cm^2\,s^{-1}}$) in SOIREE (Law et al., 2003) and $0.54\,\mathrm{cm^2\,s^{-1}}$ ($\pm 0.77\,\mathrm{cm^2\,s^{-1}}$) in EisenEx (Goldson, 2004). For SOIREE, the vertical diffusive flux of DIC ($\Delta\mathrm{DIC_{VDif}}$) into the upper 50 m was estimated from the DIC gradient between 50 and 90 m depth (Bakker et al., 2001). In EisenEx, the flux was calculated from the DIC gradient between 80% of the mixed layer depth and 120 m depth. The diffusive flux into the patch and the patch centre was calculated as the sum and the average of the flux at the individual grid points, respectively. The DIC change by vertical diffusion over time was calculated by interpolation of the flux between successive mapping periods. The error in $\Delta\mathrm{DIC_{VDif}}$ was taken as the sum of the uncertainties in K_z and from the mapping scenario.

2.8.4. Horizontal dispersion

Horizontal dispersion increased the size of the patch at a rate of $0.07\,\mathrm{day^{-1}}$ ($\pm 0.03\,\mathrm{day^{-1}}$) in SOIREE (Abraham et al., 2000). The rate of horizontal dispersion in EisenEx was calculated from the evolution of the patch size, as seen in surface water SF_6 (method courtesy of Anthony Kettle—UEA). A linear fit to the surface area of six SF_6 patches (A, in $\mathrm{km^2}$) over time (t, in days) has the equation:

$$A = 48.9t + 63.7 \qquad (3)$$

($r^2 = 0.98$, $\sigma = 65.5\,\mathrm{km}$, $n = 6$). This fit allows estimation of the daily rate of horizontal dispersion of the patch (fraction $\mathrm{day^{-1}}$) as

$$(1/A)(\mathrm{d}A/\mathrm{d}t) = 48.9/(48.9t + 63.7). \qquad (4)$$

Horizontal dispersion did not affect the DIC budget for the patch as a whole, at least if the patch was fully constrained in the $f\mathrm{CO_2}$ maps. The effect of horizontal dispersion on DIC ($\Delta\mathrm{DIC_{HDis}}$) in the patch centre was calculated for SOIREE and EisenEx by correcting $\Delta\mathrm{DIC}_{f\mathrm{CO_2}}$ for vertical diffusion and air–sea exchange. A fit to the corrected DIC change as a function of time was multiplied with the horizontal dispersion rate. Integration of this product provided $\Delta\mathrm{DIC_{HDis}}$.

The error in ΔDIC_{HDis} was calculated as sum of the errors in the coefficients in the integral. An additional error was added for the uncertainty in the mapping scenarios.

3. Results

3.1. Hydrographic setting and carbonate chemistry in SOIREE

Stable hydrographic conditions provided an ideal setting for the SOIREE experiment. Storms after days 1 and 4 mixed the added iron across the mixed layer, which had a depth of approximately 60 m to 75 m (Law et al., 2003) (Fig 2; Table 1). The waters had homogeneous physical, chemical, and biological characteristics prior to the iron fertilisation (Boyd et al., 2000; Bakker et al., 2001).

The iron additions in SOIREE promoted a phytoplankton bloom (Boyd et al., 2000). Algal carbon uptake reduced surface water fCO_2 and DIC from 4–5 days onwards. Surface water fCO_2 decreased at a rate of 3.8 µatm day^{-1} and the iron-enriched waters became a sink for atmospheric CO_2 (Fig. 2) (Watson et al., 2000; Bakker et al., 2001). The reduction of DIC occurred evenly over the upper 50 m depth. No change in DIC was apparent below 50 m depth. After 13 days surface water fCO_2 and DIC had decreased by 32–38 µatm and 15–18 µmol kg^{-1}, respectively, relative to ambient waters (Table 1) (Bakker et al., 2001).

Maps of surface water fCO_2 highlight the evolution of a gradually stretching patch (Fig. 6) (Bakker et al., 2001). Comparison of surface water fCO_2 and SF_6 indicated a uniform fCO_2 reduction across the patch centre, a 'top hat effect' (Bakker et al., 2001). A top hat effect was also seen in the photosynthetic competency (F_v/F_m) (Boyd and Abraham, 2001). The constant rate of the fCO_2 decrease, the increase in F_v/F_m from 0.3 to 0.4, and the top hat effect in fCO_2 and F_v/F_m suggest that sufficient iron had been added to overcome iron limitation in the centre of the SOIREE patch (Bakker et al., 2001; Boyd and Abraham, 2001). The algae were growing at a maximum rate for the
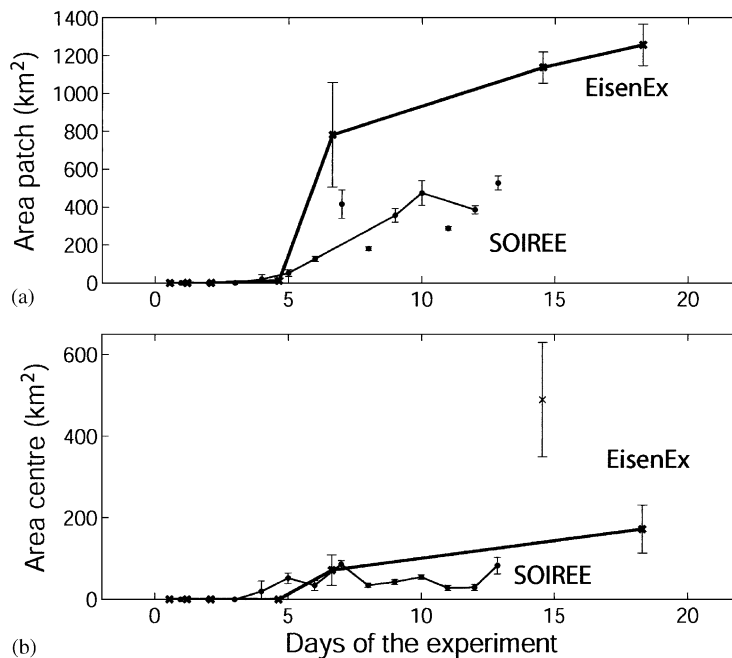

Fig. 6. (a) The size of the patch and (b) the patch centre in SOIREE (points) and EisenEx (crosses), as seen in the fCO_2 maps. Error bars indicate the uncertainty in the data, which was determined from the different mapping scenarios for SOIREE (Bakker et al., 2001) and EisenEx (Section 2).

specific environmental conditions (Bakker et al., 2001). The concentrations of nitrate, phosphate, and silicate did not become limiting during the experiment, even as silicate concentrations decreased to $7\,\mu M$ after 13 days (Boyd et al., 2000). Light limitation did not affect algal growth in the upper $65\,m$ (Boyd et al., 2000). Ocean colour observations indicated a $150\,km$ long, $4\,km$ wide SOIREE bloom, 42 days after the first iron addition (Abraham et al., 2000).

3.2. A dynamic setting and surface water fCO_2 changes in EisenEx

A succession of calm, sunny spells and strong winds dominated the EisenEx experiment with severe storms after 5 and 13 days (Fig. 3; Table 1). Deep mixing occurred during storms, while shallow stratification and surface warming took place during calm spells (Fig. 3) (Cisewski et al., 2005). Initially high horizontal dispersion of $43\%\,day^{-1}$ decreased to $14\%\,day^{-1}$ after 6 days, and to $5\%\,day^{-1}$ after 18 days (Eq. (4)). The major nutrients, nitrate, phosphate, and silicate, were not limiting during the experiment (Bozec et al., 2005). Severe light limitation of algal growth due to heavy cloud cover was present on a few days (Gervais et al., 2002).

A small reduction of surface water fCO_2 may have occurred in the EisenEx patch within 5 days (Fig. 3). Then 2 days with gale to storm-force winds doubled the mixed layer depth from $44\,m$ after 5 days to $76\,m$ after 7 days and reduced sea surface temperature by an average $0.6\,°C$ (Fig. 3). The storm strongly enlarged the patch, as seen in SF_6 (Watson et al., 2001). Any extra algal biomass and fCO_2 reduction in the iron-enriched waters would have been diluted with ambient water by deep mixing and horizontal dispersion.

Surface water fCO_2 remained relatively constant for several days after the storm (Fig. 3). A small fCO_2 decrease in the iron-enriched waters is apparent after 7 days (Fig. 4). The patch is irregular in shape, both in fCO_2 and SF_6. Between 8 and 12 days surface water fCO_2 decreased at a fairly uniform rate in the patch (Fig. 3). Surface water warming and shallowing of the mixed layer to $15–60\,m$ depth occurred in this period of low to moderate wind speed (Fig. 3). After 12 days, surface water fCO_2 in the patch was about $18\,\mu atm$ below the ambient value. A top hat effect may have occurred in the patch centre between 4 and 12 days, but disappeared after that (Fig. 7). A top hat effect in the first 12 days lends support to the hypothesis of algal growth at a rate close to the maximum rate in the centre of the EisenEx patch.
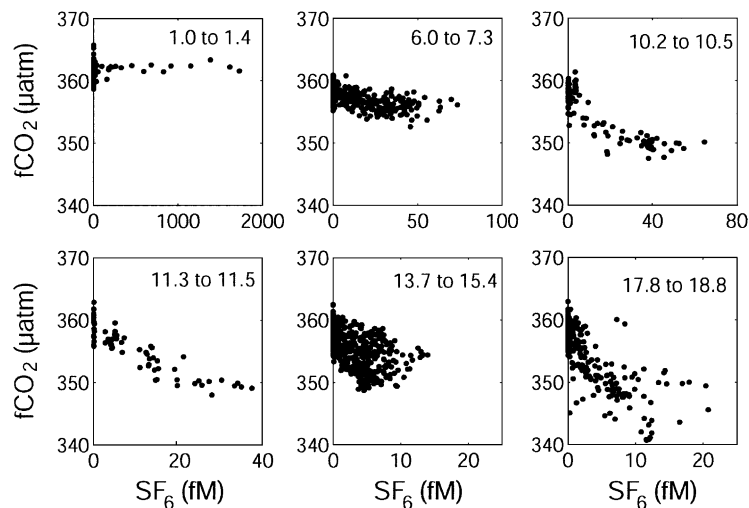

Fig. 7. Surface water fCO_2 as a function of SF_6 for different periods in EisenEx. The timing of the data is in each graph (in days).

After 12 days, another storm doubled the mixed layer depth from 40 to 90 m. Mixed layer deepening and horizontal dispersion reduced the fCO_2 anomaly in the iron-enriched waters from 18 to 10 µatm (Fig. 3). After this second storm the mixed layer depth varied between 80 and 100 m. Surface water fCO_2 in the patch gradually decreased. The fCO_2 reduction reached 20 µatm after 21 days (Fig. 3). Surface water fCO_2 maps for this period show a patch, irregular in shape, expanding in size, and rotating clockwise in the eddy (Figs. 4 and 6). As algal biomass and the mixed layer depth increased, light limitation may have developed occasionally (Gervais et al., 2002).

3.3. Atmospheric fCO_2 and CO_2 air–sea transfer in EisenEx

The mixing ratio of CO_2 in dry air (xCO_2) was relatively constant at 368.0 µmol mol^{-1} ($\sigma = 0.6$ µmol mol^{-1}) during EisenEx. Atmospheric mixing ratios of 367.6–367.8 µmol mol^{-1} were observed at Cape Point (34°21′S, 18°29′E), Crozet (46°27′S, 51°51′E), Syowa station (69°00′S, 39°35′E), and Halley Bay (75°35′S, 26°30′W) in November 2000 (WDCGG, 2003; data courtesy of C. Labuschagne, E.G. Brunke, G. Coetzee (South African Weather Service, Stellenbosch), T.J. Conway, and P.P. Tans (National Oceanographic and Atmospheric Administration—Climate Monitoring and Diagnostics Laboratory, Boulder, Colorado, USA)). The good correspondence between the EisenEx and the WDCGG data demonstrates the almost constant atmospheric CO_2 mixing ratio over large distances in subantarctic and Antarctic air.

Air–sea transfer of CO_2 in EisenEx reflects the variation in wind speed, atmospheric pressure, and surface water fCO_2. The effect of changes in atmospheric pressure between 985.6 and 1030.1 mbar (1 mbar = 10^2 Pa) on the fCO_2 air–sea

gradient (17 µatm) was of a similar magnitude as the reduction in surface water fCO_2 upon iron fertilisation (20 µatm) (Fig. 3). Ambient waters had surface water fCO_2 close to the atmospheric value and had little overall CO_2 air–sea transfer. The iron-enriched waters became a sink for atmospheric CO_2. Oceanic CO_2 uptake in the patch occasionally exceeded 10 mmol m^{-2} d^{-1} from 5 days onwards, when gale to storm-force winds coincided with air–sea fCO_2 gradients of 8–20 µatm.

3.4. Processes acting on DIC in EisenEx

Correction of the net DIC change (ΔDIC_{fCO_2}) in the iron-enriched waters, for DIC changes by horizontal dispersion (ΔDIC_{HDis}), vertical diffusion (ΔDIC_{VDif}) and CO_2 air–sea exchange (ΔDIC_{AirSea}) allows calculation of the DIC change by biological activity or net community production (ΔDIC_{NCP}) with Eqs. (5) and (6):

$$\Delta DIC_{NCP} = \Delta DIC_{fCO_2} - \Delta DICV_{Dif} - \Delta DIC_{AirSea} \qquad \text{(patch)}, \qquad (5)$$

$$\Delta DIC_{NCP} = \Delta DIC_{fCO_2} - \Delta DIC_{VDif} - \Delta DIC_{AirSea} - \Delta DIC_{HDis} \qquad \text{(patch centre)} \qquad (6)$$

(after Bakker et al., 2001). The terms in the right-hand side of the equations have been calculated for the mixed layer of the patch and the patch centre from the surface water fCO_2 maps, as described in Section 2. Unfortunately, few surface water fCO_2 maps are available for the EisenEx patch (Fig. 4). The uncertainty in ΔDIC_{NCP} in the patch and the patch centre has been calculated as the sum of the uncertainty of the terms in Eqs. (5) and (6), respectively.

The net DIC reduction (ΔDIC_{fCO_2}) across the mixed layer of the patch increased five-fold from 519 ton C (1 ton = 10^6 g) after 7 days to 2840 ton C after 18 days, while the patch increased in size from 781 to 1257 km^2 (Fig. 6; Table 5). Both the DIC reduction and the size of the EisenEx patch may well have continued to increase after 18 days. Vertical diffusion and air–sea exchange added similar, relatively small amounts of DIC to the mixed layer of the iron-enriched waters (6% each

Table 5
Changes in DIC across the patch in SOIREE (Bakker et al., 2001) and EisenEx (this study)

		SOIREE 12.0 days	EisenEx 12.0 days	EisenEx 18.3 days
Area	km^2	$387 \pm 6\%$	$1022 \pm 7\%$	$1257 \pm 6\%$
ΔDIC_{fCO_2}	10^6 g C	$-1353 \pm 6\%$	$-1236 \pm 15\%$	$-2840 \pm 15\%$
ΔDIC_{VDif}	10^6 g C	16 (-100% to 103%)	87 (-100% to 157%)	196 (-100% to $+158\%$)
ΔDIC_{AirSea}	10^6 g C	$20 \pm 52\%$	$111 \pm 58\%$	$180 \pm 56\%$
ΔDIC_{NCP}	10^6 g C	$-1389 \pm 10\%$	$-1433 \pm 27\%$	$-3217 \pm 26\%$
$\Delta DIC_{NCP}/\Delta Fe$	$mol\,mol^{-1}$	-3.7×10^3	-4.3×10^3	-6.4×10^3

The DIC uptake by net community production (ΔDIC_{NCP}) was calculated by correction of the net DIC reduction (ΔDIC_{fCO_2}) for changes by vertical diffusion (ΔDIC_{VDif}) and CO_2 air–sea exchange (ΔDIC_{AirSea}) (Eq. (3)). The EisenEx values for 12.0 days were obtained by linear interpolation.
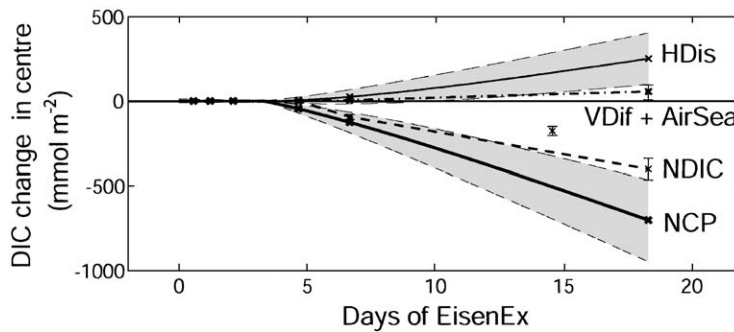

Fig. 8. Average changes in DIC for the mixed layer of the patch centre during EisenEx. The crosses mark data points, which were based on the fCO_2 maps. The dashed line indicates the net DIC change (ΔDIC_{fCO_2}, here NDIC). The dashed–dotted line corresponds to the joint supply of DIC by vertical diffusion (ΔDIC_{VDif}) and CO_2 air–sea exchange (ΔDIC_{AirSea}). The thin line indicates the supply of DIC to the patch centre by horizontal dispersion (ΔDIC_{HDis}). These terms allow calculation of DIC uptake by net community production (ΔDIC_{NCP}) (thick line) with Eq, (6). Error bars and grey shaded areas indicate the uncertainty in the estimates, which results from the uncertainty in the mapping scenario, the gas transfer velocity, the vertical diffusivity, and the rate of horizontal dispersion (Section 2).

of ΔDIC_{NCP}). From the above, we calculated a biological carbon uptake of 3217 ton C after 18 days (Fig. 9; Table 5).

The net DIC reduction (ΔDIC_{fCO_2}) in the patch centre increased from $94\,mmol\,m^{-2}$ after 7 days to $402\,mmol\,m^{-2}$ after 18 days, while the patch centre expanded in size from 72 to $172\,km^2$ (Figs. 6 and 8; Table 6). The large surface area of and the low DIC change in the patch centre after 15 days were probably artefacts of a partial mismatch between SF_6 and fCO_2 (Turner et al., 2005). These data for 15 days were excluded from the calculation of DIC changes by horizontal dispersion and biological activity in the patch centre. The method allows calculation of the biological DIC uptake in the patch

centre, if the rate of algal carbon uptake exceeded the horizontal dispersion rate. As a result, the method probably underestimates algal carbon uptake in the initial stages of EisenEx, which had high horizontal dispersion (Eq. (4)). Horizontal dispersion had diluted the biological DIC change in the patch centre ($702\,mmol\,m^{-2}$) by 36% after 18 days.

4. Discussion

4.1. Changes in DIC for SOIREE and EisenEx

The evolution of biological DIC uptake and CO_2 air–sea exchange in the patch and the patch

Table 6
Average changes in DIC in the patch centre for SOIREE and EisenEx

		SOIREE 12.0 days	EisenEx 12.0 days	EisenEx 18.3 days
$\Delta f\mathrm{CO_2}$	µatm	−32 to –38 (1)	−13 to −18	−13 to −18
ΔDIC 0–20 m	µmol kg^{-1}	−15 to −18 (1)	−12 (2)	−9 (2)
Area	km^2	29 ± 27%	118[#] ± 37%	172 ± 33%
ΔDIC$_{f\mathrm{CO_2}}$	mmol m^2	−624 ± 4%	−235[#] ± 16%	−402 ± 16%
ΔDIC$_{\mathrm{VDif}}$	mmol m^2	7 (−100% to 103%)	9# (−100% to 157%)	18 (−100% to 157%)
ΔDIC$_{\mathrm{AirSea}}$	mmol m^2	17 ± 52%	20[#] ± 55%	38 ± 54%
ΔDIC$_{\mathrm{HDis}}$	mmol m^2	189 ± 74%	115[#] ± 83%	251 ± 60%
ΔDIC$_{\mathrm{NCP}}$	mmol m^2	−837 ± 21%	−377[#] ± 42%	−702 ± 37%

The DIC change by net community production (ΔDIC$_{\mathrm{NCP}}$) was calculated by correction of the net DIC change (ΔDIC$_{f\mathrm{CO_2}}$) for changes by vertical diffusion (ΔDIC$_{\mathrm{VDif}}$), CO_2 air–sea exchange (ΔDIC$_{\mathrm{AirSea}}$) and horizontal dispersion (ΔDIC$_{\mathrm{HDis}}$) (Eq. (4)). The terms in Eq. (4) do not quite add up to the value of ΔDIC$_{\mathrm{NCP}}$, as a result of the fitting procedure for ΔDIC$_{\mathrm{HDis}}$ (Section 2). Some EisenEx values for 12 days were calculated by linear interpolation ([#]). References are: (1) Bakker et al.; (2) Bozec et al. (2005).

centre will be compared for both experiments with the objective to assess how they were affected by the contrasting mixing regimes. For EisenEx, the available data were linearly interpolated to 12 days, as indicated by a hash (#). This interpolation does not reflect reality, as it neglects the impact of the second storm.

The patch expanded in size from 4 to 5 days onwards in the experiments (Fig. 6). After 12 days, the EisenEx patch (1022 km$^{2\#}$) was more than twice the size of the SOIREE patch (387 km^2) (Table 5). The patch continued to grow in size for at least another 6 days in EisenEx and for 30 days in SOIREE (Abraham et al., 2000). The patch centre did not increase much in size after its first appearance in the experiments (Fig. 6), which suggests that a balance was soon reached between horizontal dispersion and algal carbon uptake. The patch centre in EisenEx (118 km$^{2\#}$) was 4 times larger than that in SOIREE (29 km^2) after 12 days (Table 6). The large dimensions of the patch and the patch centre in EisenEx reflect the initially strong horizontal dispersion.

After 12 days, vertical diffusion and air–sea exchange had added 4–5 times more DIC to the mixed layer of the patch in EisenEx than in SOIREE (Table 5), as a result of the higher vertical diffusivity (Table 3) and stronger winds after 5 days in EisenEx (Figs. 2 and 3). The evolution of biological DIC uptake (ΔDIC$_{\mathrm{NCP}}$) in both experimental patches was strikingly similar

with initial DIC uptake after 4–5 days (Fig. 9; Table 5). The total biological DIC reduction after 12 days was comparable in SOIREE (1389 ton C ± 10%) and EisenEx (1433 ton C[#] ± 27%), despite differences in surface water $f\mathrm{CO_2}$, the size of the patch, and the mixed layer depth. The ratio of biological DIC uptake to iron added was 3.7×10^3 mol mol^{-1} in SOIREE and -4.3×10^3 mol mol^{-1} in EisenEx (Table 5).

The average, net DIC reduction in the patch centre in SOIREE (624 mmol m^{-2}) strongly exceeded that in EisenEx (235 mmol m$^{-2\#}$) after 12 days (Table 6). Vertical diffusion and air–sea exchange had added small amounts of DIC to the mixed layer. Horizontal diffusion had lowered the biological DIC change by 23% in SOIREE and by 31% in EisenEx. Biological DIC uptake in the patch centre in SOIREE (837 mmol m^{-2}) was twice that in EisenEx (377 mmol m^{-2}) (Fig. 9).

Biological DIC uptake can be compared to the rate of carbon-14 uptake, which is often taken as an indicator for net primary productivity. These ^{14}C uptake rates have not been corrected for horizontal dispersion. In SOIREE, ^{14}C uptake in the upper 65 m of the patch centre increased from 26 to 92 mmol C m^{-2} d^{-1} over 13 days (from Gall et al. (2001) upon correction with a factor 12/14). In EisenEx ^{14}C uptake changed from 17 to 58 mmol m^{-2} d^{-1} after 12 days (Gervais et al., 2002). Both ^{14}C uptake and biological DIC reduction in the patch centre differed by a factor
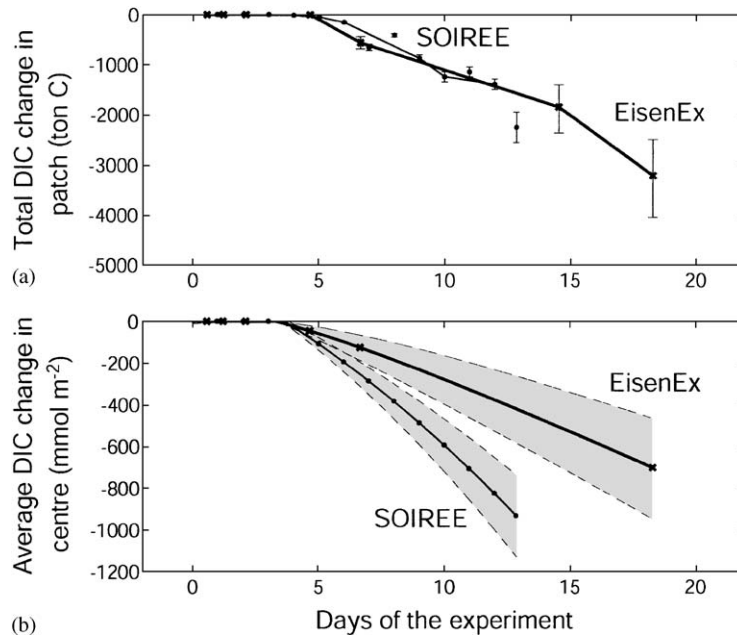
Fig. 9. The DIC reduction by net community production (ΔDIC_{NCP}) in (a) the patch and (b) the patch centre during SOIREE (points) and EisenEx (crosses). Grey shaded areas show the uncertainty in the estimates, which results from the uncertainty in the mapping scenario, the gas transfer velocity, the vertical diffusivity, and the rate of horizontal dispersion (Section 2).

of 2 between the experiments after 12 days. The high initial horizontal dispersion in EisenEx was a major factor in the reduction of ^{14}C uptake and biological DIC uptake in the centre of the EisenEx patch relative to SOIREE.

4.2. Different estimates for the net DIC reduction in EisenEx

Bozec et al. (2005) obtain $1232 \, mmol \, m^{-2}$ for the net DIC reduction in the centre of the EisenEx patch after 20 days, three-fold higher than the value of $402 \, mmol \, m^2$ ($\pm 16\%$) after 18 days in this study (Table 6). Here we compare the values. The estimates differ by 2 days in a period, when surface water DIC in the patch centre decreased by $1–3 \, \mu mol \, kg^{-1} \, day^{-1}$ (Bozec et al., 2005). Furthermore, Bozec et al. report the maximum DIC reduction, while this study presents the average reduction in the patch centre, at a time when the DIC reduction was no longer uniform across the centre (Fig. 7). Finally, Bozec et al. assume

uniform DIC uptake across the mixed layer, while a factor of 0.8 is used here.

Bozec et al. (2005) calculate a net DIC reduction of 13×10^3 ton C across the EisenEx patch after 20 days, four times more than our estimate of 2840 ton ($\pm 15\%$) for 18 days (Table 5). The discrepancy results from the aforementioned assumptions for the patch centre, as well as from a high DIC reduction of $10 \, \mu mol \, kg^{-1}$ and a 100 m deep mixed layer across the edge of the patch ($750 \, km^2$) in Bozec et al. (2005).

5. Conclusion

Two iron enrichment experiments in the Southern Ocean had a different evolution of surface water fCO_2, largely as a result of contrasting mixing regimes (Figs. 2 and 3; Table 1). Surface water fCO_2 decreased at a regular rate in SOIREE, while its evolution resembled a saw tooth in EisenEx. The SOIREE experiment was a textbook

example of algal response and biogeochemical changes upon alleviation of iron limitation.

The hydrographic and meteorological settings of the experiments were characteristic for the regions and seasons in which the experiments were carried out (Boyd et al. (2000)—on SOIREE). Moderate to high wind speeds and homogenous water properties were encountered south of the APF in late summer during SOIREE. The rapid passage of weather systems and presence of eddies, which dominated EisenEx, are typical for the area between the Subantarctic Front and the APF, south of Africa.

Biological activity had taken up comparable amounts of DIC across the experimental patches after 12 days. It seems possible that the similar amount of iron added (Table 1), as well as algal growth at a comparable near-maximum growth rate, determined the size of the biological DIC uptake across the patches, despite differences in algal composition, water temperature, insolation, mixed layer depth, and grazing pressure. Horizontal dispersion strongly affected the vertically integrated biological DIC uptake in the patch centres, but would have had little effect on the overall biological carbon uptake across the patches. The different mixing regimes had less effect on the overall biological DIC uptake across the patches than suggested by the evolution of surface water fCO_2.

By analogy, some natural algal blooms may differ less in their overall biological carbon uptake than a comparison of algal densities and surface water fCO_2 changes suggests. This only holds true, if algal carbon uptake rates are similar, algal carbon uptake dominates DIC changes, and algal density does not influence the evolution of the algal bloom, e.g. by coagulation of particles or by attracting grazers.

The iron additions made the fertilised waters sinks for atmospheric CO_2. Replenishment of CO_2 by air–sea exchange was small in comparison to algal carbon uptake. The EisenEx bloom was four times more 'efficient' than the SOIREE bloom in drawing down atmospheric CO_2 (Table 5), as a result of a higher proportion of strong winds in EisenEx from 5 days onwards. Algal growth and biological carbon uptake continued, as the ships

left the SOIREE and EisenEx sites after 12 and 22 days, respectively. No change in carbon export was observed in SOIREE (Charette and Buesseler, 2000; Nodder and Waite, 2001). An increase in carbon export may have occurred in EisenEx (Riebesell, personal communication). It is impossible to determine the fate of both blooms and how much carbon eventually left the surface ocean, thus creating a non-permanent oceanic sink for atmospheric CO_2.

In addition to more efficient uptake of atmospheric CO_2, the waters of the EisenEx area had a shorter north–south travel distance to subduction sites north of the Subantarctic Front than at the SOIREE site. As surface water at these sites sinks and mixes with deeper water to become Subantarctic Mode Water and Antarctic Intermediate Water (Sloyan and Rintoul, 2001), the EisenEx area has a better potential for storing atmospheric CO_2 and transporting carbon away from the sea surface than the SOIREE site.

The factor four difference between the estimates of the net DIC uptake based on the same data set (this study; Bozec et al., 2005) demonstrates how difficult it is to quantify the short-term biological carbon uptake upon iron fertilisation during an intensive field campaign. The uncertainty in the values becomes even larger if proxies such as chlorophyll are used for estimating carbon uptake (e.g. Abraham et al., 2000; Boyd et al., 2000). Accurate quantification of carbon export is even more demanding. The difficulty in determining carbon storage upon iron fertilisation (Gnanadesikan et al., 2003) and the low efficiency of carbon export are fundamental obstacles for the application of the method with the purpose of carbon storage.

References

Abraham, E.R., Law, C.S., Boyd, P.W., Lavender, S.J., Maldonado, M.T., Bowie, A.R., 2000. Importance of stirring in the development of an iron fertilized phytoplankton bloom. Nature 407, 727–730.

Baar, H.J.W. de, 2001. Production of iron fertilizer batches in seawater. Berichte zur Polar- und Meeresforschung 400, 145–148.

Baar, H.J.W., Boyd, P.W., 2000. The role of iron in plankton ecology and carbon dioxide transfer of the global oceans. In: Hanson, R.B., Ducklow, H.W.de, Field, J.G. (Eds.), The changing ocean carbon cycle. A midterm synthesis of the Joint Global Ocean Flux Study. International Geosphere—Biosphere Programme Book Series. Cambridge University Press, Cambridge, pp. 61–140.

Bailey, T.C., Gatrell, A.C., 1995. Interactive Spatial Data Analysis. Addison Wesley Longman Limited, Harlow, UK 413pp.

Bakker, D.C.E., Watson, A.J., Law, C.S., 2001. Southern Ocean iron enrichment promotes inorganic carbon drawdown. Deep-Sea Research Part II 48, 2483–2507.

Bowie, A.R., Maldonado, M.T., Frew, R.D., Croot, P.L., Achterberg, E.P., Mantoura, R.F.C., Worsfold, P.J., Law, C.S., Boyd, P.W., 2001. The fate of added iron during a mesoscale fertilisation experiment in the Southern Ocean. Deep-Sea Research Part II 48, 2703–2743.

Boyd, P.W., Abraham, E.R., 2001. Iron mediated changes in phytoplankton photosynthetic competence during SOIREE. Deep-Sea Research Part II 48, 2529–2550.

Boyd, P.W., Watson, A.J., Law, C.S., Abraham, E.R., Trull, T., Murdoch, R., Bakker, D.C.E., Bowie, A.R., Buesseler, K.O., Chang, H., Charette, M.A., Croot, P., Downing, K., Frew, R.D., Gall, M., Hadfield, M., Hall, J.A., Harvey, M., Jameson, G., LaRoche, J., Liddicoat, M.I., Ling, R., Maldonado, M., McKay, R.M., Nodder, S.D., Pickmere, S., Pridmore, R., Rintoul, S., Safi, K., Sutton, P., Strzepek, R., Tanneberger, K., Turner, S.M., Waite, A., Zeldis, J., 2000. A mesoscale phytoplankton bloom in the polar Southern Ocean stimulated by iron fertilization. Nature 407, 695–702.

Boyd, P.W., Law, C.S., Wong, C.S., Nojiri, Y., Tsuda, A., Levasseur, M., Takeda, S., Rivkin, R., Harrison, P.J., Strzepek, R., Gower, J., McKay, R.M., Abraham, E., Arychuk, M., Barwell-Clarke, J., Crawford, W., Crawford, D., Hale, M., Harada, K., Johnson, K., Kiyosawa, H., Kudo, I., Marchetti, A., Miller, W., Needoba, J., Nishioka, J., Ogawa, H., Page, J., Robert, M., Saito, H., Sastri, A., Sherry, N., Soutar, T., Sutherland, N., Taira, Y., Whitney, F., Wong, S.K.E., Yoshimura, T., 2004. The decline and fate of an iron-induced subarctic phytoplankton bloom. Nature 428, 549–553.

Bozec, Y., Bakker, D.C.E., Hartmann, C., Thomas, H., Bellerby, R.G.J., Nightingale, P.D., Riebesell, U., Watson, A.J., de Baar, H.J.W., 2005. The CO_2 system in a Redfield context during an iron enrichment experiment in the Southern Ocean. Marine Chemistry, doi:10.1016/j.marchem.2004.08.004, in press.

Buesseler, K.O., Andrew, J., Pike, S., Charette, M.A., 2004. The effects of iron fertilization on carbon sequestration in the Southern Ocean. Science 304, 414–417.

Charette, M.A., Buesseler, K.O., 2000. Does iron fertilization lead to rapid carbon export in the Southern Ocean? Geochemistry, Geophysics, Geosystems 1, 2000GC000069.

Chisholm, S.W., Falkowski, P.G., Cullen, J.J., 2001. Discrediting ocean fertilization. Science 294, 309–310.

Chuck, A.L., 2002. Biogenic halocarbons and light alkyl nitrates in the marine environment. Ph.D. Thesis, University of East Anglia, Norwich, 200pp.

Chuck, A.L., Turner, S.M., Liss, P.S., 2002. Direct evidence for a marine source of C_1 and C_2 alkyl nitrates. Science 297, 1151–1154.

Cisewski, B., Strass, V.H., Prandke, H., 2005. Upper ocean vertical mixing in the Antarctic Polar Front Zone. Deep-Sea Research, accepted.

Coale, K.H., Johnson, K.S., Chavez, F.P., Buesseler, K.O., Barber, R.T., Brzezinski, M.A., Cochlan, W.P., Millero, F.J., Falkowski, P.G., Bauer, J.E., Wanninkhof, R.H., Kudela, R.M., Altabet, M.A., Hales, B.E., Takahashi, T., Landry, M.R., Bidigare, R.R., Wang, X., Chase, Z., Strutton, P.G., Friederich, G.E., Gorbunov, M.Y., Lance, V.P., Hilting, A.K., Hiscock, M.R., Demarest, M., Hiscock, W.T., Sullivan, K.F., Tanner, S.J., Gordon, R.M., Hunter, C.N., Elrod, V.A., Fitzwater, S.E., Jones, J.L., Tozzi, S., Koblizek, M., Roberts, A.E., Herndon, J., Brewster, J., Ladizinsky, N., Smith, G., Cooper, D., Timothy, D., Brown, S.L., Selph, K.E., Sheridan, C.C., Twining, B.S., Johnson, Z.I., 2004. Southern Ocean iron enrichment experiment: carbon cycling in high- and low-Si waters. Science 304, 408–414.

DOE, 1994. Handbook of methods for the analysis of the various parameters of the carbon system in sea water; version 2. In: Dickson, A.G., Goyet, C. (Eds.), ORNL/CDIAC 74.

ETOPO 5, 1988. Digital relief of the surface of the earth. Data Announcement 88-MGG-02. National Oceanographic and Atmospheric Administration, National Geophysical Data Center, Boulder, CO, USA.

Fuhrman, J.A., Capone, D.G., 1991. Possible biogeochemical consequences of ocean fertilization. Limnology and Oceanography 36, 1951–1959.

Gall, M.P., Strzepek, R., Maldonado, M., Boyd, P.W., 2001. Phytoplankton processes. Part 2: rates of primary production and factors controlling algal growth during the Southern Ocean Iron RElease Experiment (SOIREE). Deep-Sea Research Part II 48, 2571–2590.

Gervais, F., Riebesell, U., Gorbunov, M.Y., 2002. Changes in the size-fractionated primary productivity and chlorophyll a in response to iron fertilization in the southern Polar Frontal Zone. Limnology and Oceanography 47, 1324–1335.

Gnanadesikan, A., Sarmiento, J.L., Slater, R.D., 2003. Effects of patchy ocean fertilization on atmospheric carbon dioxide and biological production. Global Biogeochemical Cycles 17, 1050.

Goldson, L., 2004. Vertical mixing across the seasonal pycnocline of the Southern Ocean: studies using sulphur hexafluoride tracer. Ph.D. Thesis, University of East Anglia, Norwich, UK, 219pp.

Jin, X., Gruber, N., 2003. Offsetting the radiative benefit of ocean iron fertilization by enhancing ocean N_2O emissions. Geophysical Research Letters 30 (24), 2249.

Johnson, K.M., Wills, K.D., Butler, D.B., Johnson, W.K., Wong, C.S., 1993. The performance of an automated continuous gas extractor and coulometric detector. Marine Chemistry 44, 167–188.

Journel, A.G., Huijbregts, Ch.J., 1977. Mining Geostatistics, seventh ed. Academic Press, London 600pp.

Large, W.G., Pond, S., 1981. Open ocean momentum flux measurements in moderate to strong winds. Journal of Physical Oceanography 11, 324–336.

Law, C.S., Ling, R., 2001. Nitrous oxide flux and response to increased iron availability in the Antarctic Circumpolar Current. Deep-Sea Research Part II 48, 2509–2527.

Law, C.S., Abraham, E.R., Watson, A.J., Liddicoat, M.I., 2003. Vertical diffusion and nutrient supply to the surface mixed layer in the Antarctic Circumpolar Current. Journal of Geophysical Research 108, 3272.

Liss, P.S., Merlivat, L., 1986. Air–sea exchange rates: introduction and synthesis. In: Buat-Ménard, P. (Ed.), The Role of Air–Sea Exchange in Geochemical Cycling. D. Reidel Publishing Company, Dordrecht, The Netherlands, pp. 113–127.

Martin, J.M., 1990. Glacial to interglacial CO_2 change: the iron hypothesis. Paleoceanography 5, 1–13.

Nightingale, P.D., Malin, G., Law, C.S., Watson, A.J., Liss, P.S., Liddicoat, M.I., Boutin, J., Upstill-Goddard, R.C.,

2000. In-situ evaluation of air–sea gas exchange parameterisations using novel conservative and volatile tracers. Global Biogeochemical Cycles 14 (1), 373–387.

Nodder, S.D., Waite, A.M., 2001. Is Southern Ocean organic carbon and biogenic silica export enhanced by iron stimulated increases in biological production? Sediment trap results from SOIREE. Deep-Sea Research Part II 48, 2681–2701.

Orsi, A.H., Whitworth III, T., Nowling Jr., W.D., 1995. On the meridional extent and fronts of the Antarctic Circumpolar Current. Deep-Sea Research Part I 42, 641–673.

Sloyan, B.M., Rintoul, S.R., 2001. Circulation, renewal and modification of Antarctic Mode and Intermediate Water. Journal of Physical Oceanography 31, 1005–1030.

Smetacek, V., 2001. EisenEx: International team conducts iron experiment in Southern Ocean. US JGOFS News January 11, 14.

Strass, V.H., Leach, H., Cisewski, B., Gonzalez, S., Post, J., da Silva Duarte, V., Trumm, F., 2001. The physical setting of the Southern Ocean iron fertilization experiment. Berichte zur Polar- und Meeresforschung 400, 94–130.

Takahashi, T., Olafsson, J., Goddard, J.G., Chipman, D.W., Sutherland, S.C., 1993. Seasonal variation of CO_2 and nutrients in the high-latitude surface oceans: a comparative study. Global Biogeochemical Cycles 7, 843–878.

Turner, S.M., Bakker, D.C.E., Goldson, L.E., Messias, M.J., Nightingale, P.D., 2005. Considerations on the use of sulfur hexafluoride as a deliberate tracer in oceanic biogeochemical lagrangian studies: lessons from EisenEx. In preparation for submission to Geophysical Research Letters.

Turner, S.M., Nightingale, P.D., Spokes, L.J., Liddicoat, M.I., Liss, P.S., 1996. Increased dimethyl sulphide concentrations in seawater from in situ iron enrichment. Nature 383, 513–517.

Turner, S.M., Harvey, M.J., Law, C.S., Nightingale, P.D., Liss, P.S., 2004. Iron induced changes in oceanic sulfur biogeochemistry. Geophysical Research Letters 31, L14307.

Wanninkhof, R.H., 1992. Relationship between wind speed and gas exchange over the ocean. Journal of Geophysical Research 97, 7373–7382.

Wanninkhof, R., McGillis, W.R., 1999. A cubic relationship between air–sea CO_2 exchange and wind speed. Geophysical Research Letters 26 (13), 1889–1892.

Watson, A.J., Bakker, D.C.E., Boyd, P.W., Ridgwell, A.J., Law, C.S., 2000. Effect of iron supply on Southern Ocean CO_2 uptake and implications for glacial atmospheric CO_2. Nature 407, 730–733.

Watson, A.J., Messias, M.-J., Goldson, L., Skjelvan, I., Nightingale, P., Liddicoat, M.I., 2001. SF_6 measurements on EisenEx. Berichte zur Polar- und Meeresforschung 400, 76–81.

WDCGG, 2003. World Data Centre for Greenhouse Gases of the World Meteorological Organisation. Japan Meteorological Agency, Tokyo, Japan, Online data set, http://gaw.kishou.go.jp/wdcgg/wdcgg.html.